Astron. Astrophys. 354, 86–98 (2000)

ASTRONOMY AND ASTROPHYSICS

Oscillations of a rotating star: a non-perturbative theory

Boris Dintrans[1] **and Michel Rieutord**[1,2]

[1] Laboratoire d'Astrophysique de Toulouse, Observatoire Midi-Pyrénées, 14 avenue E. Belin, 31400 Toulouse, France
[2] Institut Universitaire de France

Received 10 May 1999 / Accepted 16 September 1999

Abstract. Nonradial gravity modes of a $1.5M_\odot$ rotating ZAMS star are investigated using the anelastic approximation. Formulating the oscillation equations as a generalized eigenvalue problem, we first show that the usual second-order perturbative theory reaches its limits for rotation periods of about three days. Studying the rapid rotation régime, we develop a geometric formalism based on the integration of the characteristics of the governing mixed-type operator. These characteristics propagate in the star interior and the resulting web can be either ergodic (the web fills the whole domain) or periodic (the web reduces to an attractor along which characteristics focus). We further show the deep relation existing between the orbits of characteristics and the corresponding eigenmodes: *(i)* with ergodic orbits are associated regular eigenmodes which are similar to the usual gravity modes; *(ii)* with periodic orbits are associated singular eigenmodes for which the velocity diverges along the attractor. If diffusivity is taken into account, this singularity turns into internal shear layers tracing the attractor. As a consequence, the classical organization of eigenvalues along families with fixed (ℓ, n) disappears and leaves the place to an intricate low-frequency spectrum.

Key words: stars: individual: γ Doradus – stars: oscillations – stars: rotation

1. Introduction

Following the pioneering work of Ledoux (1951), the influence of the rotation on nonradial oscillations is generally achieved by the means of a perturbative theory, i.e. oscillation frequency in the co-rotating frame is written as

$$\sigma_{n\ell m} = \sigma^{(0)}_{n\ell} + C^{I}_{n\ell m}\Omega + C^{II}_{n\ell m}\Omega^2 + \mathcal{O}(\Omega^3) \qquad (1)$$

where $\sigma^{(0)}_{n\ell}$ is the unperturbated frequency of a mode with degree l and radial order n, m is the azimuthal number such that $-\ell \leq m \leq \ell$, $C^{I}_{n\ell m}$ and $C^{II}_{n\ell m}$ are two splitting coefficients depending on the non-rotating solution and Ω is the uniform rotation rate. For slowly rotating stars such as the Sun or many white dwarfs, the second-order effects of rotation are negligible leading to Zeeman-like multiplets which allow to infer both the mode degrees ℓ and the mean rotation rate Ω (see e.g. the study of the white dwarf PG 1159-035 by Winget et al. (1991)).

In the case of rapidly rotating variable stars, the observed multi-periodic spectra do not show uniform spacings and second-order (at least) effects of rotation on the splitting need to be taken into account. This was realized for instance with multiperiod β Cephei stars (Saio, 1981; Engelbrecht, 1986), δ Scuti stars (Breger et al., 1999; Pamyatnykh et al., 1999) or γ Doradus stars (Aerts & Krisciunas, 1996); the splitting coefficient $C^{II}_{n\ell m}$ being calculated from the theoretical works of Saio (1981) or Dziembowski & Goode (1992).

Another possibility, first proposed by Clement (1981), to deal with rapid rotations is the computation of eigenfrequencies with rotation terms directly inserted in the linearized dynamical equations. However, because of the spherical harmonics coupling, this leads to a large system of coupled equations which is hardly tractable. In addition, the convergence of eigenfrequencies becomes doubtful for high-order g-modes for which rotation effects are especially significant (Clement, 1998). Lee & Saio (1987), with a similar non-perturbative approach, computed the gravity eigenmodes of a 10 $M_\odot$ main-sequence star by including the Coriolis term but using only two spherical harmonics. Their main conclusion is that avoided crossings, similar to those caused by evolution effects (Aizenman et al., 1977), occur among eigenmodes as the rotation increases. In a following paper, Lee & Baraffe (1995) examined the pulsational stability of rotating OB stars by computing the nonadiabatic oscillations of a 5 $M_\odot$ and a 10 $M_\odot$ main-sequence stars still using two spherical harmonics. They also found similar avoided crossings and showed that the second-order effects of rotation are not so effective at influencing the pulsational stability of the oscillations.

In our preceding paper, Dintrans et al. (1999) (hereafter referred to as [I]) have been able to compute the gravito-inertial modes of a stably stratified rotating spherical shell with much more spherical harmonics (up to 300). Using the Boussinesq approximation (i.e. the fluid is assumed to be quasi-incompressible), the Brunt-Väisälä frequency is simply proportional to the radial distance and many mathematical results are known (Friedlander & Siegmann 1982a, b). On this problem, we discovered a new fascinating feature of rapidly rotating fluids,

Send offprint requests to: dintrans@obs-mip.fr

namely the preponderant part played by the underlying characteristics of the governing mixed-type operator. In fact, we showed that the shape of eigenfunctions are deeply connected to the characteristic orbits. When focusing occurs (i.e. characteristics can be attracted along a limit cycle), many eigenmodes shape internal discontinuities which have important spectral consequences since the classical ordering of eigenvalues with fixed (n, ℓ) disappears.

In this paper, we adopt a more realistic model based on the anelastic approximation to study the gravito-inertial oscillations of a 1.5 $M_\odot$ zero age main-sequence rotating star obtained from the evolutionary code CESAM of Morel (1997). The star parameters are: $R = 1.427 R_\odot$, $\log g = 4.304$, $\log(L/L_\odot) = 0.481$, $\log T_e = 3.805$, $X = 0.74$ and $Z = 0.02$; they correspond to those of a typical γ Doradus star. Rotation first perturbs g-modes (owing to their larger periods) therefore γ Doradus stars are among the best candidates to test the influence of rotation on stellar oscillations. Since the work of Balona et al. (1994), they have been identified as a new group of pulsating stars (see Handler & Krisciunas (1997) for a representative list and Aerts et al. (1998) for the latest observations with Hipparcos). They are located upon or just above the main sequence, near the cool border of the δ Scuti instability strip (with a mean spectral type F0V) and the observed periods of oscillations range from 0.2 d up to 3 d. Typical rotational velocities are 60 km s^{-1} (from 18 up to 185 km s^{-1}) which corresponds to mean rotation periods from 0.5 up to 4 days (e.g. 0.96 d for γ Dor, Balona et al. (1996)). Thus second-order corrections in the development (1) are not negligible, especially when $\sigma_{n\ell}^{(0)} \sim \Omega$.

The aim of this paper is first to show the limits of the second-order perturbative theory applied to a low-frequency gravity mode and then show how to compute non perturbatively the modes of oscillation of a rotating star. In Sect. 2, we present our anelastic model and the numerical methods we use to solve the associated generalized eigenvalue problem. We illustrate in Sect. 3.1 the capability of this non-standard approach by computing gravity modes without rotation. In Sect. 3.2, we start from a high-order g-mode with $\ell = 5$ and $n = 21$ and apply an increasing rotation rate through the Coriolis force. This large radial order n allows us to use asymptotic limits for the splitting coefficients $C_{n\ell m}^I$ and $C_{n\ell m}^{II}$. We then show that the difference between the true eigenfrequency and its second-order approximation gets so large for γ Doradus-like rotation régimes ($2\Omega/\sigma \sim 0.1$) that modes identification is not possible with approximated values.

Therefore, letting apart the perturbative approach, we investigate in Sect. 3.3 the case of rapid rotations through the geometrical formalism used in [I], i.e. we integrate the differential equation for the characteristics of the mixed-type operator governing the nonradial oscillations. We find both ergodic orbits, where the web of characteristics fills the whole domain, and periodic orbits, where the characteristics focus along an attractor. Computing the corresponding eigenmodes in Sect. 3.4 reveals us once again the deep relation existing between the orbits of characteristics and the shape of the associated eigenfunctions. As a consequence, the spectrum appears to be roughly divided in two parts: *(i)* one part corresponds to eigenvalues with $\sigma \gtrsim 2\Omega$ organized along families with fixed (ℓ, n, m), associated with ergodic orbits, and which may be identified as gravity modes perturbed by rotation; *(ii)* the other part corresponds to a chaotic distribution of eigenvalues with $\sigma \lesssim 2\Omega$, associated with attractors, and which may be identified as inertial modes perturbed by buoyancy. Finally, we conclude in Sect. 4 with some outlooks of our results.

2. The anelastic model

As shown in paper [I], the modes which are the most perturbed by rotation are those for which $\sigma \lesssim 2\Omega$ where σ is the mode frequency and 2Ω is the Coriolis frequency. The typical rotation period for γ Doradus-type stars is about one day which leads to $2\Omega \sim 150\,\mu$Hz. At such rotation rate, only low-frequency gravity modes are strongly modified by rotation. Since the frequency of a gravity mode decreases with increasing order n (see e.g. Unno et al. (1989)), rotation first perturbs high-order gravity modes.

Because of their low frequency, these modes propagate in quasi-hydrostatic equilibrium, i.e. with very small pressure fluctuations. This justifies the use of the anelastic approximation where pressure fluctuations hardly contribute to density fluctuations; hence, in the adiabatic limit, we have

$$\rho' = \frac{P'}{c_s^2} + \frac{N^2}{g}\rho\xi_r \simeq \frac{N^2}{g}\rho\xi_r$$

whereas the filtering of acoustic waves in the conservation of mass equation leads to

$$\mathrm{div}(\rho \boldsymbol{v}) = 0$$

Here N^2 denotes the square of the Brunt-Väisälä frequency and ξ_r the radial Lagrangian displacement. We note that a very similar approximation has been used by De Boeck et al. (1992) to study the low-frequency g-modes of non-rotating stars; this work is in fact based on the so-called subseismic approximation used in geophysics (Smylie & Rochester, 1981; Friedlander, 1985). The only difference with our anelastic model concerns the conservation of mass equation where these authors kept the term $N^2/g u_r$ coming from the time derivative $\partial\rho'/\partial t$. In fact, this term can be neglected as we will show in a following paper. Finally, the high radial order allows us to use the Cowling approximation (Cowling, 1941) where the perturbations in the gravitational potential are neglected.

Let us now choose the star's radius for the length scale, the dynamical time $\mathrm{T}_{dyn} = (R^3/GM)^{1/2}$ for the time scale and assume a time-dependence of the form $\exp(i\sigma t)$. In addition, as we shall concentrate on the effects of Coriolis force, we will discard all centrifugal effects and assume the star spherical. Then, in the adiabatic limit, the non-dimensional linearized equations for gravito-inertial eigenmodes in a co-rotating frame are given by

$$\left.\begin{array}{l} \mathrm{div}\,\boldsymbol{u}=0 \\ \lambda\boldsymbol{u}+f(\boldsymbol{e}_z\times\boldsymbol{u})=-\boldsymbol{\nabla}P'-N^2\zeta_r\boldsymbol{e}_r \\ \lambda\zeta_r=u_r \end{array}\right\} \quad (2)$$

where P' denotes the non-dimensional reduced pressure, $\boldsymbol{u}=\rho\boldsymbol{v}$ the non-dimensional momentum, $\zeta_r=\rho\xi_r$ and $\lambda=i\omega$ with $\omega=\sigma \mathrm{T}_{dyn}$. The rotation appears through the Coriolis term $f(\boldsymbol{e}_z\times\boldsymbol{u})$ where the parameter f is related to the ratio between the dynamical time scale and the rotation period as

$$f=4\pi\frac{\mathrm{T}_{dyn}}{\mathrm{T}_{rot}}=2\Omega\sqrt{\frac{R^3}{GM}} \quad (3)$$

In the solar case, we have $f_\odot\sim 10^{-2}$ whereas a typical value for rapidly rotating stars is $f\sim 10^{-1}$. For instance, the minimum rotation period observed for γ Doradus stars is of about one day. As the dynamic time scale of our test star is $\mathrm{T}_{dyn}\simeq 37$ mn, it leads to $f_{max}\approx 0.3$ which is the maximum f-value considered later on.

At the star center, we impose the regularity of the velocity and hence of the Lagrangian displacement. At the surface, things are more involved since, as suggested by De Boeck et al. (1992), the classical free surface condition $\delta P=0$ is not compatible with the anelastic approximation. This approximation indeed requires that the radial component of the Lagrangian displacement is such as $\xi_r\propto\omega^2/N^2$. As $|N^2|$ becomes very large near the surface, it means that ξ_r must vanish which is incompatible with the condition $\xi_r\sim\omega^2\xi_h$ resulting from $\delta P=0$ (ξ_h being finite and non-zero at the surface). Therefore we impose $\xi_r=0$ and then $\zeta_r=0$ at $r=1$.

2.1. Numerics

Following Rieutord (1987; 1991), we expand the momentum and radial displacement perturbations on spherical harmonics as:

$$\left\{\begin{array}{l} \boldsymbol{u}=\displaystyle\sum_{\ell=0}^{+\infty}\sum_{m=-\ell}^{+\ell} u_m^\ell(r)\boldsymbol{R}_\ell^m+v_m^\ell(r)\boldsymbol{S}_\ell^m+w_m^\ell(r)\boldsymbol{T}_\ell^m \\ \zeta_r=\displaystyle\sum_{\ell=0}^{+\infty}\sum_{m=-\ell}^{+\ell}\zeta_m^\ell(r)Y_\ell^m(\theta,\phi) \end{array}\right.$$

where $Y_\ell^m(\theta,\phi)$ denotes the normalized spherical harmonics and

$$\boldsymbol{R}_\ell^m=Y_\ell^m(\theta,\phi)\boldsymbol{e}_r,\quad \boldsymbol{S}_\ell^m=\boldsymbol{\nabla}Y_\ell^m,\quad \boldsymbol{T}_\ell^m=\boldsymbol{\nabla}\times\boldsymbol{R}_\ell^m \quad (4)$$

The radial equations coupling $u_m^\ell(r), w_m^\ell(r)$ and $\zeta_m^\ell(r)$ are obtained by projecting the vorticity equation on $\boldsymbol{R}_\ell^m$ and $\boldsymbol{T}_\ell^m$:

$$\left.\begin{array}{l} \lambda w_m^\ell=f\Big\{A_{\ell,m}\left[r\dfrac{du_m^{\ell-1}}{dr}+(2-\ell)u_m^{\ell-1}\right] \\ \qquad +A_{\ell+1,m}\left[r\dfrac{du_m^{\ell+1}}{dr}+(\ell+3)u_m^{\ell+1}\right]+i\dfrac{m}{\Lambda}w_m^\ell\Big\} \\ \lambda\left[r^2\dfrac{d^2u_m^\ell}{dr^2}+4r\dfrac{du_m^\ell}{dr}+(2-\Lambda)u_m^\ell\right]=\Lambda N^2\zeta_m^\ell+ \\ \qquad f\Big\{B_{\ell,m}\left[(\ell-1)w_m^{\ell-1}-r\dfrac{dw_m^{\ell-1}}{dr}\right] \\ \qquad -B_{\ell+1,m}\left[(\ell+2)w_m^{\ell+1}+r\dfrac{dw_m^{\ell+1}}{dr}\right] \\ \qquad +i\dfrac{m}{\Lambda}\left[r^2\dfrac{d^2u_m^\ell}{dr^2}+4r\dfrac{du_m^\ell}{dr}+(2-\Lambda)u_m^\ell\right]\Big\} \\ \lambda\zeta_m^\ell=u_m^\ell \end{array}\right\} \quad (5)$$

where $\Lambda=\ell(\ell+1)$ and

$$A_{\ell,m}=\frac{1}{\ell^2}\sqrt{\frac{\ell^2-m^2}{4\ell^2-1}}\quad;\quad B_{\ell,m}=\ell^2(\ell^2-1)A(\ell,m) \quad (6)$$

We also project the boundary conditions on spherical harmonics and obtain

$$\left\{\begin{array}{l} u_m^\ell=w_m^\ell=\zeta_m^\ell=0\quad\text{at}\quad r=0 \\ \zeta_m^\ell=0\quad\text{at}\quad r=1 \end{array}\right.$$

The system (5) may be written formally as

$$\mathcal{M}_A\boldsymbol{\psi}_m=\lambda\mathcal{M}_B\boldsymbol{\psi}_m \quad (7)$$

where λ are the complex eigenvalues associated with the eigenvectors $\boldsymbol{\psi}_m$ and $\mathcal{M}_A,\mathcal{M}_B$ denote two differential operators. The solutions can be symmetric ($\boldsymbol{\psi}_{m^+}$) or antisymmetric ($\boldsymbol{\psi}_{m^-}$) with respect to the equator as

$$\boldsymbol{\psi}_{m^+}\left|\begin{array}{l} u_m^m(r) \\ \zeta_m^m(r) \\ w_m^{m+1}(r) \\ u_m^{m+2}(r) \\ \zeta_m^{m+2}(r) \\ \vdots \end{array}\right.\quad\text{or}\quad \boldsymbol{\psi}_{m^-}\left|\begin{array}{l} w_m^m(r) \\ u_m^{m+1}(r) \\ \zeta_m^{m+1}(r) \\ w_m^{m+2}(r) \\ u_m^{m+3}(r) \\ \vdots \end{array}\right.$$

The operators $\mathcal{M}_A$ and $\mathcal{M}_B$ are discretized on a multi-domain Gauss-Lobato grid associated with Chebyshev polynomials leading to matrices of size about $L\times N_r$ where L and N_r are respectively the truncation orders on spherical harmonics and Chebyshev basis. The equilibrium Brunt-Väisälä profile $N^2(r)$ is also projected on the radial grid by the means of a cubic spline interpolation (Dierckx, 1993).

Two computations have been used to solve the generalized eigenvalue problem (7):

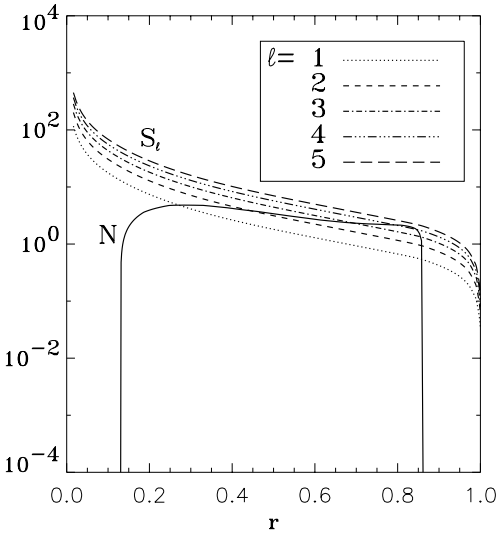

Fig. 1. Propagation diagram which gives the Brunt-Väisälä frequency profile and the Lamb frequency $S_\ell = \sqrt{\ell(\ell+1)}c_s/r$ profile for various ℓ in units of $(GM/R^3)^{1/2}$. Note the convective core which occupies about 13% of the star interior and the surface convective zone.

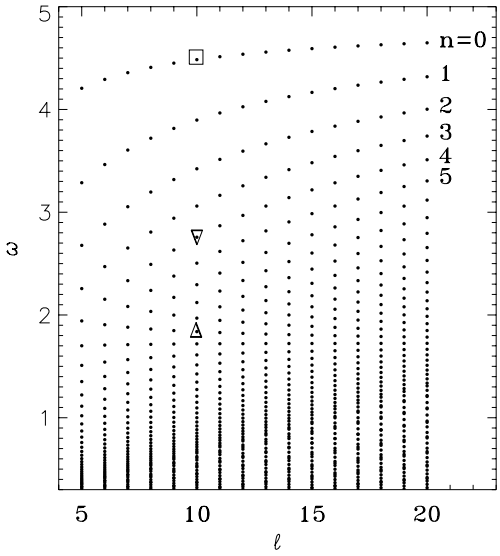

Fig. 2. Spectrum of pure gravity modes for $\ell = 5, 20$. The structures of the three modes labelled $\square$,$\triangledown$ and $\triangle$ at $\ell = 10$ are plotted in Fig. 3. The order n gives the number of nodes in the radial direction of the associated eigenvectors.

1. a direct computation based on the QZ algorithm which gives the whole spectrum of eigenvalues λ.
2. an iterative computation based on the incomplete Arnoldi-Chebyshev algorithm which gives some pairs $(\lambda, \boldsymbol{\psi}_m)$ around a given value of λ.

3. Results

3.1. Pure gravity modes and propagation diagram

A classical approach to compute nonradial p or g-modes without rotation consists in solving a two-point boundary value problem. This is achieved for instance by the means of shooting methods (Hansen & Kawaler, 1994) or relaxation methods with finite-difference equations (Osaki & Hansen, 1973; Osaki, 1975). It is only recently that the formulation of the oscillation equations as a generalized eigenvalue problem has been proposed (see e.g. Pesnell (1990) which used the secant method of Castor (1971)). For our problem where infinitely many equations are coupled, the use of shooting or relaxation methods is not convenient; we therefore preferred the generalized eigenvalue problem formulation. However, as this method has not often been used in the past, we find useful to show its capability on the standard case of gravity modes of a non-rotating star.

Without rotation, the toroidal component w_m^ℓ of the velocity along $\boldsymbol{T}_\ell^m$ decouples and the system (5) reduces to the following simple form:

$$r^2\frac{d^2\zeta_m^\ell}{dr^2} + 4r\frac{d\zeta_m^\ell}{dr} + (2-\Lambda)\zeta_m^\ell = -\Lambda\frac{N^2}{\omega^2}\zeta_m^\ell \qquad (8)$$

with boundary conditions $\zeta_m^\ell = 0$ at $r = 0$ and $r = 1$. From this second-order differential equation for ζ_m^ℓ, it is easy to show that oscillations are trapped in radiative zones between concentric spheres of radius r_0 such as $|\omega| = N(r_0)$ and, consequently, that the spectrum of pure gravity modes is bounded by N_{max}. The usual demonstration is achieved via a local analysis of a high-order mode using a WKB method (see e.g. Unno et al. (1989)). We propose in appendix (A.1) a more general demonstration based on the study of the mixed-type operator governing the global oscillations; this demonstration being later on extended to the rotating case.

However, it is well known that a second condition of trapping exists for gravity modes, namely $|\omega| < S_\ell(r)$ where S_ℓ is the Lamb frequency. As we use the anelastic approximation, this second trapping due to acoustic effects is not reproduced. Therefore, we should define a critical ℓ-value to ensure that the condition $|\omega| < S_\ell(r)$ is also verified. It is achieved by the means of the propagation diagram given by Fig. 1. We show in this diagram that $N(r) < S_\ell(r)$ for $\ell \geq 5$. As gravity modes propagate in the region $|\omega| < N(r)$, it means that the condition $|\omega| < S_\ell(r)$ is always satisfied for these ℓ and then ensures that the anelastic approximation is valid as long as the radial order n is high enough.

Fig. 2 shows the spectrum of pure gravity modes obtained by a QZ computation for $5 \leq \ell \leq 20$. As expected, the spectrum is bounded by $N_{max} \sim 4.7$. To each ℓ corresponds a set of eigenvalues which are characterized by the number of node in the radial direction of their associated eigenvectors. This is illustrated in Fig. 3 which gives the corresponding eigenvectors for the three modes labelled $\square$, $\triangledown$ and $\triangle$ in Fig. 2 at $\ell = 10$. The dimensionless mode frequencies are respectively $\omega_\square \simeq 4.485$ (first mode in the frequency order), $\omega_\triangledown \simeq 2.756$ (fourth mode) and $\omega_\triangle \simeq 1.837$ (tenth mode). The first mode has no node, the fifth mode as four nodes and the tenth mode as nine nodes; we thus recover that the number of nodes increases as the frequency decreases.

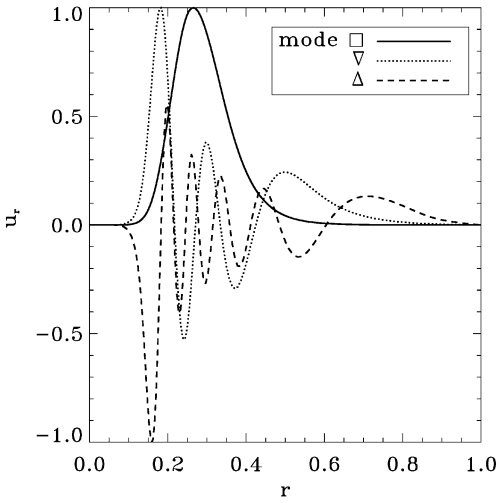

Fig. 3. Associated normalized eigenvectors for the three modes labelled □,▽ and △ at $\ell = 10$ from Fig. 2. These modes respectively admit $0, 4$ and 9 nodes in the radial direction. Note the left shifting of the eigenfunctions as the frequency decreases because the change of the turning radius r_0 given by $N(r_0) = \omega$.

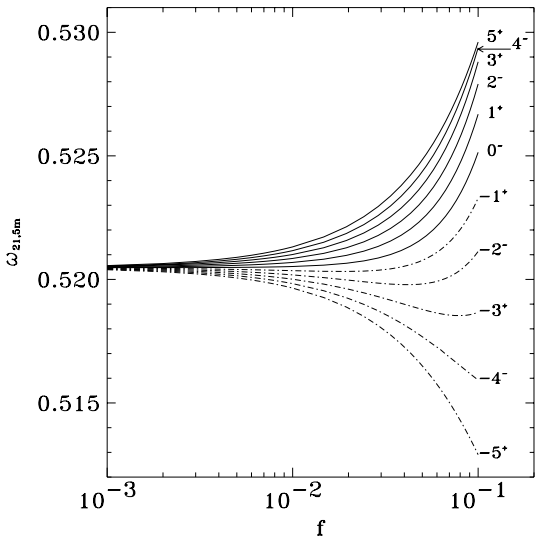

Fig. 4. Rotational splittings of the eigenvalue $\omega^{(0)}_{21,5}$ as f increases. Eleven new eigenvalues appear according to $m = 0^-, \pm1^+, \pm2^-, \pm3^+, \pm4^-, \pm5^+$.

3.2. The limits of the second-order theory

The Eq. (1) rewritten in non-dimensional form reads

$$\omega_{th} = \omega^{(0)}_{n\ell} + C_1 f + C_2 f^2 + \mathcal{O}(f^3) \tag{9}$$

where the rotation is now characterized by the free parameter f. We calculate in appendix B the splitting coefficients C_1 and C_2 by the means of a WKB theory applied to a low-frequency mode with $n \to +\infty$ and $\omega \to 0$; hence we find

$$\begin{cases} C_1 = \dfrac{m}{2\Lambda} \\ C_2 = \dfrac{1}{\omega^{(0)}_{n\ell}} \left\{ \dfrac{2\Lambda - 3}{2(4\Lambda - 3)} - m^2 \left[\dfrac{\Lambda - 3}{\Lambda(4\Lambda - 3)} + \dfrac{1}{8\Lambda^2} \right] \right\} \end{cases}$$

which are, except for a small second-order correction, the coefficients given by Chlebowski (1978)[1].

As a pedagogical example for testing the robustness of the asymptotic development (9), we have chosen a very low-frequency eigenvalue, such as $\omega^{(0)}_{n\ell} \sim 0.520$ with $\ell = 5$ and a high radial order $n = 21$. It corresponds to a gravity mode with a period $\mathrm{T}_{osc} \simeq 0.31$ d ($\nu = 37.3\,\mu$Hz). Thus, eleven new eigenvalues $\omega_{n\ell m}$ corresponding to the $2\ell + 1$ possible m-values should be observed as f increases, whereas the symmetry $+/-$ of each mode is imposed as $m = 0^-, \pm1^+, \pm2^-, \pm3^+, \pm4^-, \pm5^+$ because of the parity of the non-rotating eigenvector.

Fig. 4 shows the splitting of the non-rotating eigenvalue $\omega^{(0)}_{21,5}$ as f increases. As expected, we observe eleven new eigenvalues. Comparing these eigenvalues with the approximated ones ω_{th} predicted by (9) allows us to test the second-order perturbative theory. It is achieved in Fig. 5 where the relative errors $|\omega_{21,5m} - \omega_{th}|/\omega_{21,5m}$ have been plotted as f increases.

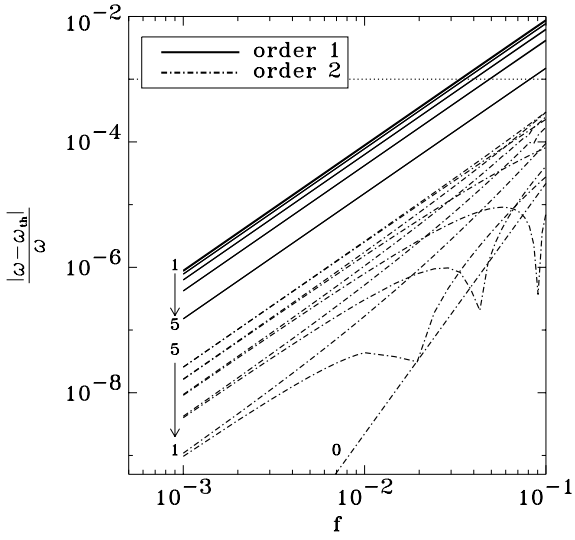

Fig. 5. Relative errors $|\omega_{21,5m} - \omega_{th}|/\omega_{21,5m}$ as the rotation increases. Here ω_{th} are the first- or second-order approximations given by the development (9) whereas $\omega \equiv \omega_{n\ell m}$ are the computed ones. The numbers denote the $|m|$-values.

We first show that the accuracy benefit induced by the second-order correction depends on the m-value. For instance at $f = 10^{-3}$, the agreement with the true eigenvalue is about a thousand times better for $|m| = 1$ when the second-order correction is taken into account. On the contrary, we just get a five times more precise theoretical eigenvalues for $|m| = 5$. In addition, we note that this accuracy difference tends to be less pronounced as the rotation increases since the precision benefit is just about one hundred times at $f = 0.1$ for $|m| = 1$ while the improvement is still by a factor 5 in the case $|m| = 5$. It means

[1] Conversely, the asymptotic formula (117) given by Dziembowski & Goode (1992) is not compatible with our results.

that among the non-axisymmetric modes, the large-scale ones (i.e. with a small m) are the most sensitive to rotation. In other words, taking into account a second-order correction leads to an improvement of the eigenvalues with small $|m|$ whereas those with large $|m|$ are not much improved.

As long as the difference between the true eigenvalues and the perturbative ones are smaller than the frequency resolution of the observations, the perturbative theory remains useful, i.e. the identification of the observed frequency with its counterpart calculated from the development (9) is possible. For instance, the expected precision on eigenfrequencies measured by the satellite COROT is about $0.1\,\mu$Hz (Michel, 1998). For a gravity mode with $\nu = 37.3\,\mu$Hz, it corresponds to a relative error of about 10^{-3}. Thus, using Fig. 5, it is clear that the first-order perturbative theory becomes rapidly inapplicable since the relative errors equal 10^{-3} for $f \sim 4\times10^{-2}$ if $|m| = 1, 2, 3, 4$ and for $f \sim 8\times10^{-2}$ if $|m| = 5$. It corresponds respectively to rotation periods of about eight and four days. As a typical rotation period is about one day for γ Doradus stars, it means that second-order corrections (at least) are necessary to understand the observed frequency splittings of these stars. We note that the case $m = 0$ is less affected since corrections are $\mathcal{O}(f^2)$.

Unfortunately, it turns out that the second-order perturbative theory also reaches its limits for γ Doradus-like rotations in the case $m \neq 0$. In fact, for $f = 0.1$ (i.e. a rotation period of about three days), the second-order approximation is in error of $\sim 5\times10^{-4}$, a value very close to COROT's precision. Thus, in order to increase once again the accuracy of the theoretical eigenvalues (this accuracy being already improved of about hundred times when second-order corrections is taken into account at $f = 0.1$), a third-order perturbative theory seems necessary for such rotations (see Soufi et al. (1998) for a first attempt in this direction). However, as shown by this latter work, developments of the third-order approximation are quite cumbersome and therefore make the use of a non-perturbative theory preferable.

3.3. The web of characteristics

Restoring the rotation into the dynamics equations dramatically complicates the mathematical side of nonradial oscillations. For instance, we have shown that pure gravity modes propagate in a domain confined between concentric spheres of radius r_0 such as $N(r_0) = \omega$. It means that we deal with a governing operator of mixed type whose turning surfaces, according to the spherical symmetry of the gravity force, are spheres. With rotation, this operator remains of mixed type but the associated critical surfaces are no longer spherical owing to the cylindrical symmetry of the Coriolis force. The equation of turning surfaces reads now (see appendix A.2 for a demonstration):

$$\omega^2 r^2 (N^2 + f^2 - \omega^2) - f^2 N^2 z^2 = 0 \tag{10}$$

In paper [I] where $N(r) \propto r$, these surfaces are either ellipsoids for $\omega > f$ or hyperboloids for $\omega < f$. In the present case, we have a more intricate profile $N(r)$ and the shape of these surfaces is more complicated. However, the classification used in [I] (i.e. the E_1, E_2, H_1 and H_2-modes) remains valid because it only depends on the spectral properties of the governing operator and not on the equilibrium profiles (except for the Brunt-Väisälä one). Thus, we define the same four types of modes but we add a tilde to emphasize that the shape of the associated critical surfaces are different:

– the $\widetilde{E}$-modes correspond to $\omega > f$ with the two sub-classes

$$\begin{aligned} &\widetilde{E}_1 : \quad f < \omega < N_{max} \\ &\widetilde{E}_2 : \max(f, N_{max}) < \omega < (f^2 + N_{max}^2)^{1/2} \end{aligned} \tag{11}$$

– the $\widetilde{H}$-modes correspond to $\omega < f$ with the two sub-classes

$$\begin{aligned} &\widetilde{H}_1 : N_{max} < \omega < f \\ &\widetilde{H}_2 : 0 < \omega < \min(f, N_{max}) \end{aligned} \tag{12}$$

In an astrophysical context, it is clear that the $\widetilde{H}_1$-modes cannot exist because $f < N_{max}$. In fact, with the Brunt-Väisälä profile given by Fig. 1, it turns out that the $\widetilde{H}_1$-modes would only exist with $f \gtrsim 5$ which is larger than the keplerian limit $f = 2$. In the same way, the $\widetilde{E}_2$-modes are marginal because of the narrowness of their spectral interval (i.e. $\max(f, N_{max}) = N_{max}$ and $(f^2 + N_{max}^2)^{1/2} \sim N_{max}$ for $f \lesssim 0.3$). Therefore, only the $\widetilde{H}_2$- and $\widetilde{E}_1$-modes are relevant to stars and have been studied in this paper. We note that $\widetilde{E}_1$-modes correspond to classical gravity modes more or less perturbed by rotation.

Another new mathematical feature introduced by rotation concerns the characteristics of the governing operator. With rotation, these characteristics are defined by the following differential equation (see appendix A.2):

$$\frac{dz}{ds} = \frac{N^2 sz \pm r\Gamma^{1/2}}{\omega^2 r^2 - N^2 z^2} \tag{13}$$

where Γ is given by

$$\Gamma = \omega^2 N^2 s^2 + (f^2 - \omega^2)(\omega^2 r^2 - N^2 z^2) \tag{14}$$

and (s, ϕ, z) denote the usual cylindrical coordinates. In [I], we have shown that many interesting properties of gravito-inertial modes can be deduced from the web of characteristics obtained after integrating (13). The characteristics, which reflect both on the boundaries and on the critical surfaces, indeed shape a web whose structure gives useful indications on the nature of the corresponding eigenfunctions. As the critical surfaces have presently more complicated forms, these patterns differ from those obtained in [I], especially with the $\widetilde{H}_2$-modes. However, this geometric approach keeps its relevance as it will be shown below.

Typical webs of characteristics associated with $\widetilde{H}_2$ and $\widetilde{E}_1$-modes are illustrated in Fig. 6. We first note that the characteristics trajectories are very different: those associated with an $\widetilde{H}_2$-mode propagate both in the convective and radiative zones while those associated with an $\widetilde{E}_1$-mode remain trapped in the radiative zone. As $N^2(r) \sim 0$ in convective zones, the differential equation (13) becomes

$$\frac{dz}{ds} \simeq \pm \left(\frac{f^2 - \omega^2}{\omega^2} \right)^{1/2} \tag{15}$$

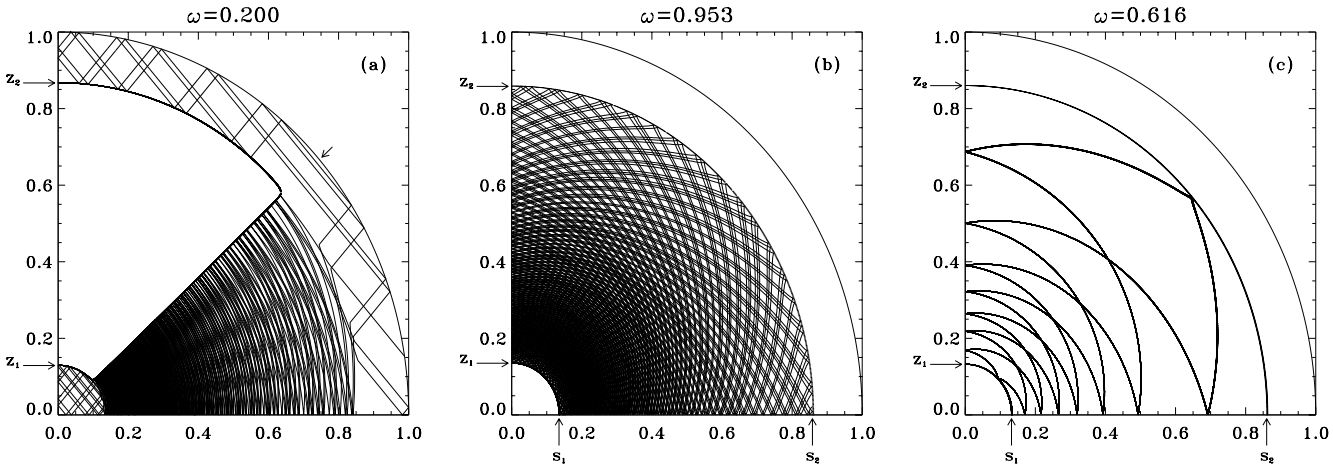

Fig. 6a–c. Webs of characteristics for a $\widetilde{H}_2$-mode **a** and two $\widetilde{E}_1$-modes **b** and **c** at a given rotation rate $f = 0.3$. The s_i and z_i locations correspond to $N(s_i) = (\omega^2 - f^2)^{1/2}$ and $N(z_i) = \omega$. The arrow on the outer sphere in **a** marks the critical latitude $\sin\theta_c = \omega/f$ of $\widetilde{H}_2$-mode. Three hundred, one hundred and two hundred reflections have been drawn respectively in plots **a**, **b** and **c** whereas the first hundred reflections in plot **c** has been removed to emphasize the final attractor.

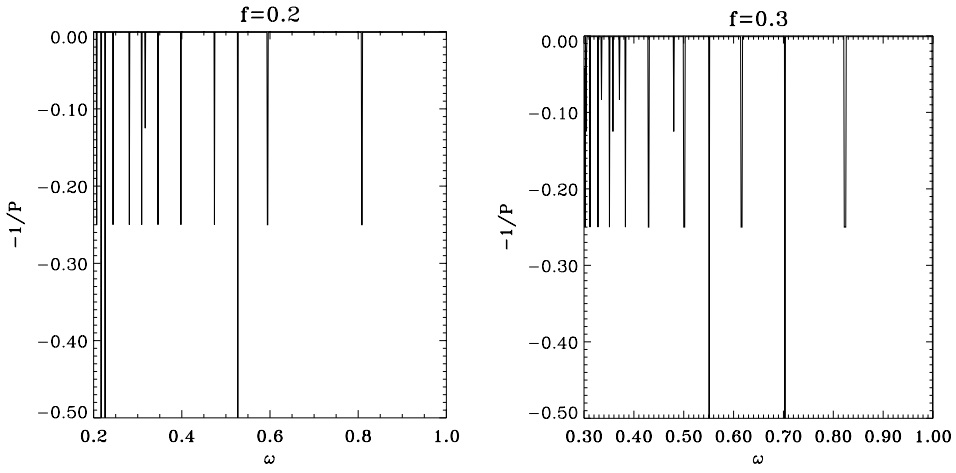

Fig. 7. Period diagrams for $f = 0.2$ and $f = 0.3$ and $\varepsilon = 10^{-5}$. Some bands of attractors appear but ergodic orbits largely dominate.

and the characteristics are straight lines as in the pure inertial case (Rieutord & Valdettaro, 1997). On the other hand, for a mode with $\omega \sim f$, the differential equation (13) takes the form

$$\frac{dz}{ds} \simeq \left(1 \pm \frac{\omega}{N}\right) \frac{sz}{\frac{\omega^2}{N^2}r^2 - z^2} \tag{16}$$

In the radiative zone and when $N \gg \omega$, this equation reduces to

$$\frac{dz}{ds} \simeq -\frac{s}{z} \tag{17}$$

which means that characteristics are almost circles as illustrated by Fig. 6a.

Following the paths of characteristics, we obtain two kinds of orbits: *(i)* ergodic orbits which fill the whole hyperbolic domain (Fig. 6b), *(ii)* periodic orbits (hereafter referred to as attractors) along which characteristics focus (Fig. 6c). In order to find all the attractors at a fixed rotation rate f, we used the period diagram introduced by Maas & Lam (1995). The period P of an orbit is defined as the smallest integer such that $|\theta_{N_0+P} - \theta_{N_0}| \leq \varepsilon$ where θ_i is the latitude of the ith-reflection point on the outer critical surface and ε a given accuracy. In practice, for each pattern, we first compute $N_0 = 1000$ reflections and iterate until the angular distance $|\theta_{N_0+P} - \theta_{N_0}|$ is less than or equal to $\varepsilon = 10^{-5}$, with a maximum of $P_m = 1000$ reflections. If the characteristics do not focus along a limit cycle then the period of the orbit is set equal to P_m whereas a lower period value means that focusing occurs. We note that the period and the length of an attractor are in fact the same. In addition, we have shown that the characteristics are almost circles in the radiative zone if $\omega \sim f$. Hence, the periods associated with $\widetilde{H}_2$-modes (i.e. $0 < \omega < \min(f, N_{max})$) are always very long and this is why only periods of $\widetilde{E}_1$-modes have been computed.

Fig. 7 shows the period diagrams obtained for two values of the rotation rate f, says $f = 0.2$ ($\mathrm{T}_{rot} \simeq 1.6$ d) and $f = 0.3$ ($\mathrm{T}_{rot} \simeq 1$ d). As in Maas & Lam (1995), we have chosen to plot $-1/P$ instead of P to make the connection with the Lyapunov exponents computed in [I]. We obtain respectively 19 and 28 bands of periodic orbits for $f = 0.2$ and $f = 0.3$ for which $P < P_m$. Thus increasing the rotation deforms more and

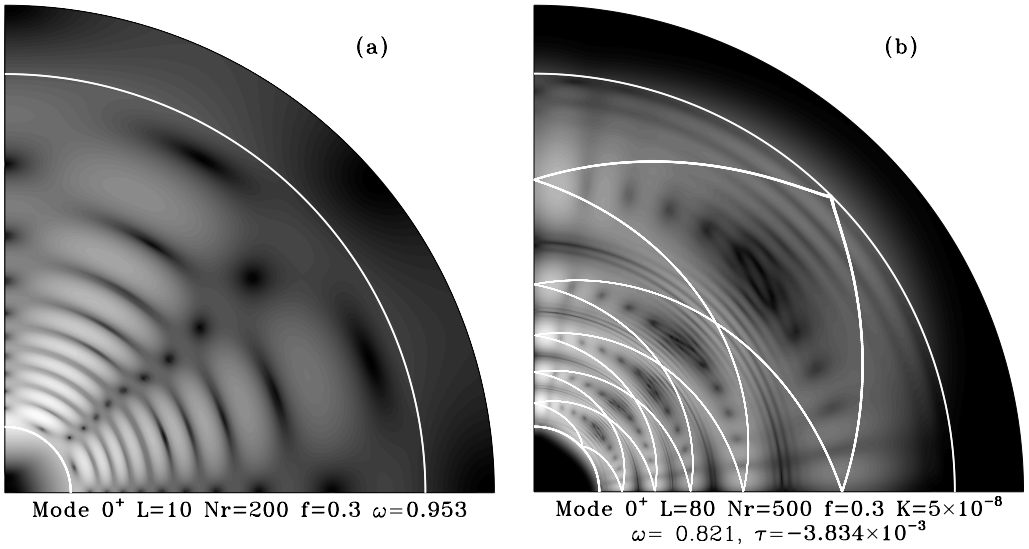

Fig. 8a and b. Meridional sections of kinetic energy for two axisymmetric $\widetilde{E}_1$- modes ($m = 0^+$,$f = 0.3$) whom the orbit of characteristics is either ergodic **a** or periodic **b**; the superimposed white lines showing the theoretical attractor in this latest case. To the ergodic orbit corresponds a regular eigenmode computable with low resolutions and without diffusion. On the contrary, a singular mode is associated with the periodic orbit and its computation requires the use of thermal diffusivity with large resolutions which leads to internal shear layers following the attractor.

more the critical surfaces and the probability of focusing also increases. It is indeed important to note that no focusing occurs in the non-rotating case; that is, all the orbits of pure gravity modes are ergodic[2].

In these bands, all the orbits show the focusing of characteristics along a limit cycle as illustrated by Fig. 6c. The largest band we found is the one centered around $\omega \simeq 0.825$ for $f = 0.3$, with width $\sim 10^{-3}$. The narrowness of these bands has important consequences as will be shown below. In addition, Fig. 7 shows that attractors concentrate around the frequency $\omega \sim f$. It suggests that only the low-frequency part of the spectrum is concerned by geometric focusing; a result already found in [I]. As a consequence, most of the orbits which are not in the régime $\omega \lesssim f$ seem to remain ergodic as shown in Fig. 7.

3.4. Relation with eigenmodes

We have found, with the characteristic paths, that two kinds of orbits are possible: the first case corresponds to ergodic orbits which fill the whole hyperbolic domain whereas the second one corresponds to periodic orbits tracing attractors. In addition, the period diagrams have shown that the ergodic orbits are the most numerous. The last step consists in determining the relation between the orbits of characteristics and the eigenmodes solutions of the generalized eigenvalue problem (7).

The easiest case corresponds to ergodic orbits. As no focusing occurs for the characteristics, the associated eigenfunctions do not have to deal with any geometric constraint, except that of matching of the critical surfaces. Therefore, as in [I], these ergodic orbits should be associated with regular eigenmodes, i.e. with a smooth square-integrable velocity field. Fig. 8a shows a good example of this association between ergodic orbits and regular eigenmodes. We have represented the kinetic energy distribution in a meridional plane for an axisymmetric $\widetilde{E}_1$-mode with $\omega \simeq 0.953$ and $f = 0.3$. At this frequency, we show in Fig. 6b and Fig. 7 that the underlying characteristics are ergodic. It means that an ergodic orbit leads to a regular eigenmode or, in other words, to a smooth velocity field without any discontinuity. We note that this result could be inferred from the non-rotating case since, as mentionned above, we found that a space-filling web of characteristics is associated with every computed gravity mode.

However, this correspondence between ergodic orbits and regular eigenmodes fails with the $\widetilde{H}_2$-modes. In this case, the hyperbolic domain can be separated in three independent regions (see Fig. 6a):

- a first convective zone near the center. In fact, this region can be seen as a full unstratified sphere where pure inertial modes propagate. Since the work of Bryan (1889), we know that eigenmodes exist in this configuration and are probably associated with ergodic orbits (Rieutord et al., 1999).
- a radiative zone. Gravito-inertial modes propagate in this stably stratified shell and the orbits of the almost circular characteristics are either ergodic or periodic with very long periods. Hence, regular modes associated with ergodic orbits may exist.
- a second convective region below the surface. As near the center, inertial modes propagate once again while being now confined in a spherical shell. This new geometry (a shell instead of a full sphere) strongly changes the physics since, apart from a set of purely toroidal modes no inertial modes exist in the adiabatic limit for this configuration (Rieutord et al., 1999) because all orbits focus more or less rapidly along an attractor.

[2] We cannot exclude the possibility of strictly periodic orbits for which characteristics exactly fold back upon themselves; however, this kind of orbit has not been observed; either in the rotating or non-rotating case.

Thus, it is clear that the surface convective zone sets a problem in the case of $\widetilde{H}_2$-modes. Starting from a regular eigenfunction associated with an ergodic orbit at the center, it is possible to find at the same frequency a regular eigenfunction with an ergodic orbit in the radiative zone. At this stage, we deal with a resonant coupling between an inertial mode and a gravity-like mode; this phenomenon being already observed by Lee & Saio (1987) in the case of a 10 $M_\odot$ main-sequence star. But, as no regular eigenmode can be found near the surface, a global smooth eigenfunction existing in the whole domain is not possible. As a consequence, computation of global adiabatic $\widetilde{H}_2$-eigenmodes is not possible.

Finally, modes associated with attractors are necessarily singular with non square-integrable velocity fields. Maas & Lam (1995), studying the propagation of pure gravity modes in a two-dimensional parabolic basin, have shown that as the characteristics converge towards an attractor, the spatial scale of the associated function (here the streamfunction) tends to zero while keeping a constant amplitude. In our case, the equation of characteristics (13) has been also derived from the streamfunction operator which means that the spatial scale of the streamfunction field also decreases as the limit cycle is approached. As $\boldsymbol{u} \propto \boldsymbol{\nabla}\psi$, it means that the velocity diverges along the attractor and that the computation of the associated eigenmode is not possible without diffusion.

Therefore, we have taken into account the radiative damping of the eulerian temperature perturbations T' which, in the anelastic approximation, are related to the eulerian density perturbations ρ' by

$$\rho' = -\delta\frac{\rho}{T}T' \quad ; \quad \delta = \left(\frac{\partial \ln P}{\partial \ln T}\right)_\rho \left(\frac{\partial \ln P}{\partial \ln \rho}\right)_T^{-1}$$

and T' satisfies the following energy equation

$$\lambda T' + \frac{N^2}{\beta}u_r = \mathcal{K}\nabla^2 T' \quad ; \quad \beta = \delta\frac{\rho g}{T} \tag{18}$$

where we have neglected the derivative of the thermal diffusivity $\mathcal{K} = (4ac/3\kappa\rho)T^3$ (κ being the opacity). Restoring thermal diffusivity leads to internal shear layers tracing the periodic orbit, that is the growth of the velocity along the attractor is hindered by diffusive effects. If we suppose, as obtained in [I], that these shear layers scale with $\mathcal{K}^{1/4}$ then the frequency variations due to the radiative damping would be $\propto \mathcal{K}^{1/2}$. As seen in Sect. 3.3, the largest width of periodic orbit bands is $\sim 10^{-3}$; it means that these periodic modes will appear only if $\mathcal{K} \lesssim 10^{-6}$. Above this critical value, attractors cannot be detected. As in stars $\mathcal{K} \sim 10^{-12}$ in the radiative zone, attractors may exist but their computations are presently not feasible because of the needed resolution. We thus choose to take $\mathcal{K} = 5\times10^{-8}$ which allows us to both emphasize attractors and use an acceptable resolution.

Fig. 8b shows the obtained $\widetilde{E}_1$ axisymmetric eigenmode for $f = 0.3$ and $\omega \simeq 0.821$. As given by the period diagram at $f = 0.3$ in Fig. 7, the characteristics focus along an attractor at this frequency. With diffusivity, this attractor yields internal shear layers which are well reproduced in the kinetic energy distribution. Then, as with the ergodic orbits, we obtain a direct correspondence between the periodic orbits and the associated eigenmodes with diffusion.

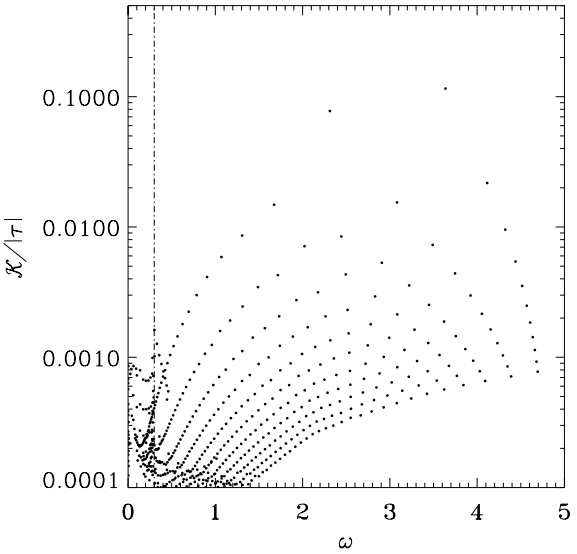

Fig. 9. Distribution in the complex plane $(\omega, \mathcal{K}/|\tau|)$ of the eigenvalues with $f = 0.3$, $m = 0^+$ and $\mathcal{K} = 5\times10^{-5}$. The resolution is $L = 22$ and $Nr = 100$.

Finally, let us come back to the spectrum of gravito-inertial modes. Using the QZ algorithm, we computed the whole eigenvalue spectrum in the axisymmetric case $m = 0^+$ with $f = 0.3$ and $\mathcal{K} = 5\times10^{-5}$. This high $\mathcal{K}$-value has been necessary to compute eigenvalues with reasonable precision (QZ method leading to large full matrices). Fig. 9 shows the obtained eigenvalue distribution in the complex plane $(\omega, \mathcal{K}/|\tau|)$.

We first note that the spectrum is bounded by $(N_{max}^2 + f^2)^{1/2} \sim N_{max} \simeq 4.7$; this limit being in fact almost the same than those deduced from the spectrum of pure gravity mode in Fig. 2. In addition, we also find again the same organization of eigenvalues along branches with fixed ℓ in the region $\omega > f$; the location of an eigenvalue in a branch still depends on the number of nodes in the radial direction of its associated eigenvector. Therefore, we show that $\widetilde{E}_1$-modes associated with ergodic orbits behave like gravity modes; the only differences being the new frequency range $[f, N_{max}]$ instead of $[0, N_{max}]$ and the existence of some singular eigenmodes due to attractors. We note moreover that the attractors bands are not visible in the spectrum (especially the largest around $\omega \sim 0.825$) because the thermal diffusivity $\mathcal{K}$ is too high.

In fact, the main modification of the spectrum concerns $\widetilde{H}_2$-modes with $\omega < f$. For these frequencies, eigenvalues are not distributed along families which means that the 2D-organization with fixed (ℓ, n) is destroyed. We have shown that $\widetilde{H}_2$-modes are not regular in the surface convective zone and restoring diffusion leads to internal shear layers. As a consequence, we cannot associate a well defined ℓ-value with these eigenstructures and the corresponding highly-damped eigenvalues are now randomly distributed in the low-frequency part of the spectrum.

4. Conclusions

We have computed the gravito-inertial modes of a $1.5M_\odot$ rotating ZAMS star using the anelastic approximation. Restoring the rotation into the dynamic equations through the Coriolis force, we formulate the nonradial oscillation equations as a generalized eigenvalue problem. Thus we have both studied the low rotation régime with $2\Omega \ll \sigma$ and the rapid rotation one with $2\Omega \sim \sigma$ where Ω denotes the uniform rotation rate and σ the eigenfrequency.

Starting from a low-frequency gravity eigenmode and slowly increasing the rotation, we have first shown that the usual second-order perturbative theory reaches its limits for rotation periods of about three days. Thus, in order to study more precisely the rapid rotation régime, we have developed a geometric approach based on the integration of the characteristics of the governing mixed-type operator. To the two types of modes which are astrophysically relevant correspond two kinds of orbits: *(i)* ergodic orbits which fill the whole hyperbolic domain, *(ii)* periodic orbits for which characteristics focus along an attractor. Computing the corresponding eigenmodes, we have proved the direct relation existing between the orbit type and the shape of the eigenfunctions:

- with ergodic orbits are associated regular eigenmodes, in the sense that the velocity field is smooth and square-integrable. It is the case with the ergodic $\widetilde{E}_1$-orbits ($\omega > f$) but not with the $\widetilde{H}_2$-ones ($\omega < f$).
- with periodic orbits are associated singular eigenmodes with no square-integrable velocity field. In fact, as the characteristics converge towards the attractor, the spatial scale of the streamfunction field rapidly decreases which means that the velocity diverges along the periodic orbit. Hence, computations of eigenmodes associated with attractors require the use of a radiative damping to smooth out the singularities of the velocity field. Its leads to internal shear layers tracing the attractor. Decreasing the thermal diffusivity also decreases the width of these shear layers therefore, as the adiabatic limit is taken, the shear layers are reduced to a simple line corresponding to the final limit cycle for the characteristics. Hence, the amplitude of the velocity field tends to infinity and no physical eigenmodes survive; i.e. the point spectrum of the operator may be empty in the subintervals corresponding to attractors.

Concerning the spectrum of gravito-inertial modes, its shape depends on the presence of diffusivity. In the limit of zero diffusivity, only the $\widetilde{E}_1$-eigenmodes associated with ergodic orbits may remain because of the vanishing of $\widetilde{H}_2$-modes ($\omega < f$) and $\widetilde{E}_1$-modes corresponding to attractors. With diffusivity, the ergodic $\widetilde{E}_1$-modes are the least-damped ones whereas those associated with attractors and the $\widetilde{H}_2$-modes are highly damped because of the small scales generated by internal shear layers aligned along the attractors. Hence, the spectrum is divided in two parts: *(i)* eigenvalues which both are in $[f, N_{max}]$ and correspond to ergodic orbits are distributed along families with fixed (ℓ, n, m), *(ii)* those associated with attractors (some in $[f, N_{max}]$ and those in $[0, f]$) are randomly distributed.

Finally, the above results have direct astrophysical applications as far as eigenmodes associated with ergodic or periodic orbits are concerned. For instance, it is clear that regular $\widetilde{E}_1$-modes are the best candidates to explain the large scale oscillations of rapidly rotating stars. In fact, $\widetilde{E}_1$-modes with ergodic orbits behave similarly as the usual gravity modes. Eigenvalues seem to be easily identifiable since the 2D-organization with fixed (ℓ, n) remains valid.

In the case of singular $\widetilde{E}_1$ or $\widetilde{H}_2$-modes associated with attractors, things are more involved. With diffusivity, these eigenmodes shape internal shear layers along the attractors leading to a high damping. Hence, these singular modes are promising vectors of angular momentum or chemical elements when the nonlinear régime is considered. Gravito-inertial waves have been already suspected to play an important part in the angular momentum redistribution in star's interiors (Lee & Saio, 1993; Kumar et al., 1999). But regular eigenfunctions have been always invoked as support of this transport. Because very small scales are generated along the attractors, singular modes would be more efficient to transfer angular momentum; an application in this direction will be developed in a forthcoming paper.

Acknowledgements. We first thank Pierre Morel for letting us use his stellar structure code CESAM and Lorenzo Valdettaro for his collaboration in the numerical part of this work. We also thank C. Catala, J.-P. Zahn, G. Berthomieu and J. Provost for many fruitful discussions. Most of the calculations have been carried out on the Cray C98 and Fujitsu VP300 of the Institut du Développement et des Ressources en Informatique Scientifique (IDRIS) which is gratefully acknowledged.

Appendix A: properties of the mixed-type governing operator

A.1. Case without rotation: pure gravity modes

In this appendix, we derive the second-order differential equation for the meridional streamfunction of pure gravity modes and recover that oscillations are trapped between concentric spheres and the spectrum is bounded by N_{max}. We start from the system (2) by eliminating the Coriolis term:

$$\begin{cases} \text{div}\, \boldsymbol{u} = 0 \\ \\ i\omega \boldsymbol{u} = -\boldsymbol{\nabla} P' - N^2 \zeta_r \boldsymbol{e}_r \\ \\ i\omega \zeta_r = u_r \end{cases}$$

where we have substituted λ with $i\omega$. We consider axisymmetric modes (i.e. $\partial_\phi = 0$) and introduce the meridional streamfunction $\psi(s,z)$ such as

$$\boldsymbol{u} = \overrightarrow{Rot}\left(\frac{\psi}{s}\boldsymbol{e}_\phi\right) + u_\phi(s,z)\boldsymbol{e}_\phi \qquad \text{(A.1)}$$

where (s, ϕ, z) are the usual cylindrical coordinates. Then, taking the ϕ-component of the curl of the momentum equation, we

obtain

$$-i\omega\nabla^2\left(\frac{\psi}{s}\boldsymbol{e}_\phi\right) = \frac{\partial}{\partial s}(N^2\zeta_r\cos\theta) - \frac{\partial}{\partial z}(N^2\zeta_r\sin\theta) = \left(\cos\theta\frac{\partial}{\partial s} - \sin\theta\frac{\partial}{\partial z}\right)(N^2\zeta_r)$$

where θ denotes the co-latitude whereas ζ_r is related to ψ by

$$\xi_r = \frac{1}{i\omega}\frac{1}{s}\left(\cos\theta\frac{\partial}{\partial s} - \sin\theta\frac{\partial}{\partial z}\right)\psi$$

Substituting ξ_r, we obtain the following equation for the streamfunction alone

$$\frac{\partial^2\psi}{\partial s^2} - \frac{1}{s}\frac{\partial\psi}{\partial s} + \frac{\partial^2\psi}{\partial z^2} = s\left(\cos\theta\frac{\partial}{\partial s} - \sin\theta\frac{\partial}{\partial z}\right) \times\left[\frac{N^2}{\omega^2}\frac{1}{s}\left(\cos\theta\frac{\partial}{\partial s} - \sin\theta\frac{\partial}{\partial z}\right)\psi\right] \tag{A.2}$$

As the type of a differential operator only depends on their leading order derivatives (see e.g. Zwillinger (1992)), we rewrite (A.2) keeping second-order derivative terms only:

$$(\omega^2 - N^2\cos^2\theta)\frac{\partial^2\psi}{\partial s^2} + 2N^2\cos\theta\sin\theta\frac{\partial^2\psi}{\partial s\partial z} +(\omega^2 - N^2\sin^2\theta)\frac{\partial^2\psi}{\partial z^2} + F\left(\frac{\partial\psi}{\partial s},\frac{\partial\psi}{\partial z},\psi\right) = 0 \tag{A.3}$$

This operator changes type on the critical surface $\Gamma = 0$ where Γ is defined by

$$\Gamma = \omega^2 r^2(N^2 - \omega^2) \tag{A.4}$$

and pure gravity modes only propagate in the hyperbolic domain defined by $\Gamma > 0$ (they are evanescent in the elliptic domain $\Gamma < 0$). As a consequence, the oscillations are trapped between concentric spheres of radius r_0 such as $N(r_0) = |\omega|$ and the spectrum of pure gravity modes is bounded by N_{max}.

A.2. Case with rotation: gravito-inertial modes

In this appendix, we calculate the new form of the governing mixed-type operator when rotation is taken into account and show how the critical surfaces and spectrum are modified compared to the non-rotating case. We start from the full system (2) with the Coriolis term:

$$\left\{\begin{array}{l}\mathrm{div}\,\boldsymbol{u} = 0\\ i\omega\boldsymbol{u} + f(\boldsymbol{e}_z\times\boldsymbol{u}) = -\boldsymbol{\nabla}P' - N^2\zeta_r\boldsymbol{e}_r\\ i\omega\zeta_r = u_r\end{array}\right. \tag{A.5}$$

and restrict, as above, our attention to axisymmetric modes. Hence, the equation verified by the meridional streamfunction ψ (already defined in A.1) is given by

$$\frac{\partial^2\psi}{\partial s^2} - \frac{1}{s}\frac{\partial\psi}{\partial s} + \left(1 - \frac{f^2}{\omega^2}\right)\frac{\partial^2\psi}{\partial z^2} = s\left(\cos\theta\frac{\partial}{\partial s} - \sin\theta\frac{\partial}{\partial z}\right)\left[\frac{N^2}{\omega^2}\frac{1}{s}\left(\cos\theta\frac{\partial}{\partial s} - \sin\theta\frac{\partial}{\partial z}\right)\psi\right] \tag{A.6}$$

whereas taking the leading order terms leads to

$$(\omega^2 - N^2\cos^2\theta)\frac{\partial^2\psi}{\partial s^2} + 2N^2\cos\theta\sin\theta\frac{\partial^2\psi}{\partial s\partial z} +(\omega^2 - f^2 - N^2\sin^2\theta)\frac{\partial^2\psi}{\partial z^2} + G\left(\frac{\partial\psi}{\partial s},\frac{\partial\psi}{\partial z},\psi\right) = 0 \tag{A.7}$$

As expected by the cylindrical symmetry of the Coriolis force, we note that the only differences with the non-rotating case come from terms $\propto \partial^2/\partial z^2$. Hence, the function Γ defining the turning surfaces on which the operator changes type is now given by

$$\Gamma = \omega^2 r^2(N^2 + f^2 - \omega^2) - f^2N^2z^2 \tag{A.8}$$

It is then clear that the critical surfaces are no longer spherical as for pure gravity modes owing to the new term $-f^2N^2z^2$. Setting to zero this term shows in addition that the spectrum with rotation is bounded by $(N^2_{max} + f^2)^{1/2}$; this limit being larger than those obtained in the non-rotating case. In the hyperbolic domain, a pair of real characteristics propagate following the differential equation

$$\frac{dz}{ds} = \frac{N^2sz \pm r\Gamma^{1/2}}{\omega^2r^2 - N^2z^2} \tag{A.9}$$

Finally, we note that introducing an angular dependence of the form $\exp(im\phi)$ leads to the same equations for the critical surface and characteristics because the second-order terms are unchanged; the new term $\partial^2/\partial\phi^2 \equiv -m^2$ being in fact of zero derivative order.

Appendix B: A second-order perturbative theory using WKB theory

In this appendix, we calculate the second-order splitting coefficients for a low-frequency gravity mode (i.e. $n \to +\infty$ and $\sigma \to 0$) and find a small correction to the second-order coefficient given in Chlebowski (1978). We start from the following dimensional anelastic equations for $\boldsymbol{\zeta} = \rho\boldsymbol{\xi}$ and P':

$$\left.\begin{array}{l}\sigma^2\boldsymbol{\zeta} - i\sigma 2\Omega\boldsymbol{e}_z\times\boldsymbol{\zeta} = \boldsymbol{\nabla}P' + N^2\zeta_r\boldsymbol{e}_r,\\ \mathrm{div}\,\boldsymbol{\zeta} = 0\end{array}\right\} \tag{B.1}$$

We expand $\boldsymbol{\zeta}$ and P' on spherical harmonics as

$$\boldsymbol{\zeta} = a^l_m\boldsymbol{R}^m_\ell + b^l_m\boldsymbol{S}^m_\ell + c^l_m\boldsymbol{T}^m_\ell \quad ; \quad P' = p^l_mY^m_\ell$$

where $\boldsymbol{R}_\ell^m$, $\boldsymbol{S}_\ell^m$ and $\boldsymbol{T}_\ell^m$ are given by (4). Hence, the projection of Coriolis force $\boldsymbol{e}_z \times \boldsymbol{\zeta}$ reads

$$\left\{\begin{array}{l} \boldsymbol{R}_\ell^m : \dfrac{1}{\Lambda}\left[\ell B_{\ell,m} c_m^{\ell-1} - (\ell+1) B_{\ell+1,m} c_m^{\ell+1} - im\Lambda b_m^l\right] \\ \\ \boldsymbol{S}_\ell^m : \dfrac{1}{\Lambda}\left[B_{\ell,m} c_m^{\ell-1} + B_{\ell+1,m} c_m^{\ell+1} - im(a_m^l + b_m^l)\right] \\ \\ \boldsymbol{T}_\ell^m : \ell A_{\ell,m}\left[a_m^{\ell-1} - (\ell-1) b_m^{\ell-1}\right] - \\ \qquad (\ell+1) A_{\ell+1,m}\left[a_m^{\ell+1} + (\ell+2) b_m^{\ell+1}\right] - i\dfrac{m}{\Lambda} c_m^l \end{array}\right.$$

where $\Lambda = \ell(\ell+1)$ and the coefficients $A_{\ell,m}$ and $B_{\ell,m}$ are given by (6). As we deal with low-frequency gravity modes, we now apply the same hierarchy between the radial functions a_m^l, b_m^l, c_m^l and p_m^l as in Berthomieu et al. (1978); that is

$$p_m^l \ll a_m^l \ll b_m^l \sim c_m^l$$

which leads to the following coupled equations

$$\left\{\begin{array}{l} a_m^l \simeq \dfrac{1}{\sigma^2 - N^2}\dfrac{dp_m^l}{dr} \\ \\ b_m^l - \dfrac{i}{\Lambda}\dfrac{\eta}{\beta_{\ell,m}}\left(B_{\ell,m} c_m^{\ell-1} + B_{\ell+1,m} c_m^{\ell+1}\right) \simeq \dfrac{1}{\beta_{\ell,m}\sigma^2}\dfrac{p_m^l}{r} \\ \\ c_m^l \simeq -i\dfrac{\eta}{\beta_{\ell,m}}\left[\ell(\ell-1) A_{\ell,m} b_m^{\ell-1} + \right. \\ \qquad \left. (\ell+2)(\ell+1) A_{\ell+1,m} b_m^{\ell+1}\right] \\ \\ \dfrac{da_m^l}{dr} \simeq \Lambda\dfrac{b_m^l}{r} \end{array}\right.$$

where

$$\eta = \frac{2\Omega}{\sigma} \quad \text{and} \quad \beta_{\ell,m} = 1 - \frac{m}{\Lambda}\eta$$

Hence, $c_m^{\ell\pm1}$ are related to c_m^l and $c_m^{\ell\pm2}$ by

$$\left\{\begin{array}{l} c_m^{\ell-1} = -i\dfrac{\eta}{\beta_{\ell,m}}\left[(\ell-1)(\ell-2) A_{\ell-1,m} b_m^{\ell-2} + \Lambda A_{\ell,m} b_m^l\right] \\ \\ c_m^{\ell+1} = -i\dfrac{\eta}{\beta_{\ell,m}}\left[\Lambda A_{\ell+1,m} b_m^l \right. \\ \qquad \left. +(\ell+3)(\ell+2) A_{\ell+2,m} b_m^{\ell+2}\right] \end{array}\right.$$

and the couplings in the equation for b_m^l can be formally written as

$$b_m^l \propto \frac{\eta}{\beta_{\ell,m}} c_m^{\ell\pm1} \propto \left(\frac{\eta}{\beta_{\ell,m}}\right)^2 (b_m^l; b_m^{\ell\pm2}) \tag{B.2}$$

or, in the same way,

$$b_m^{\ell+2} \propto \left(\frac{\eta}{\beta_{\ell+2,m}}\right)^2 (b_m^l; b_m^{\ell+2}; b_m^{\ell+4}) \tag{B.3}$$

We then show, as in Dziembowski & Goode (1992), that the couplings $(\ell, \ell\pm2)$ only contribute to the fourth order in Ω since substituting $b_m^{\ell+2}$ in Eq. (B.2) leads to

$$b_m^l \propto \left[\left(\frac{\eta}{\beta_{\ell,m}}\right)^2 b_m^l; \frac{\eta^4}{\beta_{\ell,m}\beta_{\ell+2,m}}(b_m^l; b_m^{\ell+2}; b_m^{\ell+4})\right]$$

which means that $c_m^{\ell\pm1}$ can be approximated to second order by

$$\begin{aligned} c_m^{\ell-1} &\simeq -i\frac{\eta}{\beta_{\ell,m}}\Lambda A_{\ell,m} b_m^l \quad \text{and} \\ c_m^{\ell+1} &\simeq -i\frac{\eta}{\beta_{\ell,m}}\Lambda A_{\ell+1,m} b_m^l \end{aligned}$$

Therefore, b_m^l and p_m^l are related by

$$b_m^l = \frac{1}{\alpha_{\ell,m}\beta_{\ell,m}\sigma^2}\frac{p_m^l}{r}$$

with

$$\alpha_{\ell,m} = 1 - \left(\frac{\eta}{\beta_{\ell,m}}\right)^2 (A_{\ell,m} B_{\ell,m} + A_{\ell+1,m} B_{\ell+1,m})$$

Moreover, we have to leading order in d/dr

$$\frac{da_m^l}{dr} \simeq \frac{1}{\sigma^2 - N^2}\frac{d^2 p_m^l}{dr^2}$$

and the final equation for the pressure alone reads

$$\frac{d^2 p_m^l}{dr^2} = \frac{\Lambda}{\alpha_{\ell,m}\beta_{\ell,m}}\frac{\sigma^2 - N^2}{\sigma^2}\frac{p_m^l}{r^2} \quad ; \quad \sigma \to 0 \tag{B.4}$$

We now apply a WKB approximation for the radial function $p_m^l(r)$; that is

$$p_m^l(r) = \mathcal{A}(r)\exp i\mathcal{S}(r)/\delta \quad ; \quad \delta \to 0$$

where the amplitude $\mathcal{A}(r)$ and the phase $\mathcal{S}(r)$ are assumed to be slowly varying functions (see e.g. Bender & Orszag (1978)). Thus the WKB approximation of (B.4) is

$$\sigma^2\left(\frac{k^2}{\delta^2}\mathcal{A} - \mathcal{A}'' - 2i\frac{k}{\delta}\mathcal{A}' - i\frac{k'}{\delta}\mathcal{A}\right) = \frac{\Lambda}{\alpha_{\ell,m}\beta_{\ell,m}}\frac{N^2}{r^2}\mathcal{A}$$

where $k = d\mathcal{S}/dr$. The largest term on the left-hand side is $k^2\mathcal{A}\sigma^2/\delta^2$ and must balance the right-hand side therefore a distinguished limit is $\delta \sim \sigma$. Hence we have

$$k = \pm\left(\frac{\Lambda}{\alpha_{\ell,m}\beta_{\ell,m}}\right)^{1/2}\frac{N}{r} \quad \text{and} \quad \mathcal{A} \sim |k|^{-1/2}$$

and the phase function $\mathcal{S}(r)$ is given by

$$\mathcal{S}(r) = \pm\left(\frac{\Lambda}{\alpha_{\ell,m}\beta_{\ell,m}}\right)^{1/2}\int^r N\frac{dt}{t}$$

Thus an approximate solution for the radial function $p_m^l(r)$ is

$$p_m^l(r) \sim |k|^{-1/2}\left(\mathcal{C}_1\cos\frac{\mathcal{S}(r)}{\sigma} + \mathcal{C}_2\sin\frac{\mathcal{S}(r)}{\sigma}\right)$$

where $\mathcal{C}_1$ and $\mathcal{C}_2$ are constants to be determined by boundary conditions. If we impose $p_m^l = 0$ at $r = 0$ and $r = 1$, we have

$$p_m^l(r) \sim \mathcal{C}|k|^{-1/2} \sin \frac{\mathcal{S}(r)}{\sigma} \quad \text{with} \quad \frac{\mathcal{S}(r)}{\sigma} = n\pi$$

or, in a similar manner,

$$\pm \frac{1}{\sigma} \left(\frac{\Lambda}{\alpha_{\ell,m}\beta_{\ell,m}} \right)^{1/2} \int^r N \frac{dt}{t} = n\pi$$

where n denotes an integer. If we apply the same WKB formalism to a high-order g-mode without rotation, we obtain the following well-known quantization rule for the non-rotating frequency σ_0 (see e.g. Unno et al. (1989))

$$\sigma_0 \sim \frac{\sqrt{\Lambda}}{n\pi} \int^r N \frac{dt}{t}$$

which means that

$$\frac{\sigma}{\sigma_0} = (\alpha_{\ell,m}\beta_{\ell,m})^{-1/2}$$

Calculating the right hand-side by the means of a second-order development in Ω/σ_0 finally leads to

$$\frac{\sigma}{\sigma_0} = 1 + \frac{m}{\Lambda}\frac{\Omega}{\sigma_0} + \left\{ \frac{2(2\Lambda-3)}{4\Lambda-3} - m^2 \left[\frac{4(\Lambda-3)}{\Lambda(4\Lambda-3)} + \frac{1}{2\Lambda^2} \right] \right\} \left(\frac{\Omega}{\sigma_0} \right)^2$$

We thus recover the splitting coefficients of Chlebowski (1978) with, however, an additional second-order correction equal to $-m^2/2\Lambda^2$.

References

Aerts C., Eyer L., Kestens E., 1998, A&A 337, 790
Aerts C., Krisciunas K., 1996, MNRAS 278, 877
Aizenman M., Smeyers P., Weigert A., 1977, A&A 58, 41
Balona L.A., Böhm T., Foing B.H., et al., 1996, MNRAS 281, 1315
Balona L.A., Krisciunas K., Cousins A.W.J., 1994, MNRAS 270, 905
Bender C.M. Orszag S.A., 1978, Advanced mathematical methods for scientists and engineers. Mc Graw-Hill
Berthomieu G., Gonczi G., Graff P., Provost J., Rocca A., 1978, A&A 70, 597
Breger M., Pamyatnykh A.A., Pikall H., Garrido R., 1999, A&A 341, 151
Bryan G., 1889, Phil. Trans. R. Soc. London 180, 187
Castor J.I., 1971, ApJ 166, 109
Chlebowski T., 1978, Acta Astron. 28, 441
Clement M.J., 1981, ApJ 249, 746
Clement M.J., 1998, ApJS 116, 57
Cowling T.G., 1941, MNRAS 101, 367
De Boeck I., Van Hoolst T., Smeyers P., 1992, A&A 259, 167
Dierckx P., 1993, Curve and surface fitting with splines. Oxford University Press
Dintrans B., Rieutord M., Valdettaro L., 1999, J. Fluid Mech. 398, 271
Dziembowski W.A., Goode P.R., 1992, ApJ 394, 670
Engelbrecht C.A., 1986, MNRAS 223, 189
Friedlander S., 1985, Geophys. Astrophys. Fluid Dyn. 31, 151
Friedlander S. Siegmann W. L., 1982a, J. Fluid Mech. 114, 123
Friedlander S. Siegmann W. L., 1982b, Geophys. Astrophys. Fluid Dyn. 19, 267
Handler G., Krisciunas K., 1997, Delta Scuti Newsletter 11, 3
Hansen C.J., Kawaler S.D., 1994, Stellar interiors. Springer-Verlag
Kumar P., Talon S., Zahn J.-P., 1999, ApJ in press
Ledoux P., 1951, ApJ 114, 373
Lee U., Baraffe I., 1995, A&A 301, 419
Lee U., Saio H., 1987, MNRAS 224, 513
Lee U., Saio H., 1993, MNRAS 261, 415
Maas L., Lam F.-P., 1995, J. Fluid Mech. 300, 1
Michel E., 1998, In: Kjeldsen H., Bedding T.R. (eds.) The First MONS Workshop: Science with a Small Space Telescope. Aarhus Universitet
Morel P., 1997, A&AS 124, 597
Osaki Y., 1975, PASJ 27, 237
Osaki Y., Hansen C.J., 1973, ApJ 185, 277
Pamyatnykh A., Dziembowski W.A., Handler G., Pikall H., 1999, A&A 333, 141
Pesnell P., 1990, ApJ 363, 227
Rieutord M., 1987, Geophys. Astrophys. Fluid Dyn. 39, 163
Rieutord M., 1991, Geophys. Astrophys. Fluid Dyn. 59, 182
Rieutord M., Georgeot B., Valdettaro L., 1999, submitted to J. Fluid Mech.
Rieutord M., Valdettaro L., 1997, J. Fluid Mech. 341, 77
Saio H., 1981, ApJ 244, 299
Smylie D., Rochester M.G., 1981, Phys. Earth & Planet. Inter. 24, 308
Soufi F., Goupil M.J., Dziembowski W.A., 1998, A&A 334, 911
Unno W., Osaki Y., Ando H., Saio H., Shibahashi H., 1989, Nonradial oscillations of stars. University of Tokyo Press
Winget D.E., Nather R.E., Clemens J., et al., 1991, ApJ 378, 326
Zwillinger D., 1992, Handbook of differential equations. Academic Press